HHS Public Access

Author manuscript

J Mol Cell Cardiol. Author manuscript; available in PMC 2017 November 19.

Published in final edited form as:

J Mol Cell Cardiol. 2017 October ; 111: 27–39. doi:10.1016/j.yjmcc.2017.08.004.

Novel obscurins mediate cardiomyocyte adhesion and size via the PI3K/AKT/mTOR signaling pathway

Maegen A. Ackermann[a,b,**,1], **Brendan King**[a], **Nicole A.P. Lieberman**[a,2], **Prameela J. Bobbili**[b], **Michael Rudloff**[c], **Christopher E. Berndsen**[c], **Nathan T. Wright**[c], **Peter A. Hecker**[d], and **Aikaterini Kontrogianni-Konstantopoulos**[a,*]

[a]Department of Biochemistry and Molecular Biology, University of Maryland, School of Medicine, Baltimore, MD 21201, United States

[b]Department of Physiology and Cell Biology, Wexner College of Medicine, Dorothy M. Davis Heart and Lung Research Institute, The Ohio State University, Columbus, OH 43210, United States

[c]Department of Chemistry and Biochemistry, James Madison University, Harrisonburg, VA 22807, United States

[d]Division of Cardiology and Department of Medicine, University of Maryland, Baltimore, MD 20201, United States

Abstract

The intercalated disc of cardiac muscle embodies a highly-ordered, multifunctional network, essential for the synchronous contraction of the heart. Over 200 known proteins localize to the intercalated disc. The challenge now lies in their characterization as it relates to the coupling of neighboring cells and whole heart function. Using molecular, biochemical and imaging techniques, we characterized for the first time two small obscurin isoforms, obscurin-40 and obscurin-80, which are enriched at distinct locations of the intercalated disc. Both proteins bind specifically and directly to select phospholipids via their pleckstrin homology (PH) domain. Overexpression of either isoform or the PH-domain in cardiomyocytes results in decreased cell adhesion and size via reduced activation of the PI3K/AKT/mTOR pathway that is intimately linked to cardiac hypertrophy. In addition, obscurin-80 and obscurin-40 are significantly reduced in acute (myocardial infarction) and chronic (pressure overload) murine cardiac-stress models underscoring their key role in maintaining cardiac homeostasis. Our novel findings implicate small obscurins in the maintenance of cardiomyocyte size and coupling, and the development of heart failure by antagonizing the PI3K/AKT/mTOR pathway.

[*]Correspondence to: A. Kontrogianni-Konstantopoulos, University of Maryland School of Medicine, 108 N. Greene St., Baltimore, MD 21201, United States. [**]Correspondence to: M. A. Ackermann, The Ohio State University, 473 W. 12th Ave, Columbus, OH 43210, United States.

[1]Current Addresses: Department of Physiology and Cell Biology, Wexner College of Medicine, Dorothy M. Davis Heart and Lung Research Institute, The Ohio State University, Columbus, OH 43210, United States.

[2]Ben Towne Center for Childhood Cancer Research, Seattle Children's Research Institute, Seattle, WA 98101, United States.

Disclosures

None.

Appendix A. Supplementary data

Supplementary data to this article can be found online at http://dx.doi.org/10.1016/j.yjmcc.2017.08.004.

Keywords

Intercalated disc; Obscurin; PI3K/AKT/mTOR; Pleckstrin homology domain; Phosphatidyl-inositol bisphosphates

1. Introduction

The intercalated disc (ID) of cardiomyocytes is a unique membrane microdomain that mediates myocyte coupling through protein-protein interactions, enabling their synchronous beating. Mutations in genes encoding ID proteins affect the structural organization and integrity of the ID resulting in irregular conductance and lack of synchronicity, ultimately leading to arrhythmogenic cardiomyopathy and heart failure [1,2].

The highly organized structure of the ID is composed of gap junctions, adherens junctions, and desmosomes; however, the ID acts as a single functional unit to maintain structural integrity and synchronicity throughout the heart [3]. In addition, linkages between the ID, the contractile apparatus, and the sarcoplasmic reticulum are mediated through structural proteins at the transitional junction, a region just beyond the ID membrane [4]. With the recent advancement of proteomic technologies, new members of the ID proteome have been identified, including novel isoforms of obscurin, described herein.

Obscurins are multidomain proteins composed of adhesion modules and signaling motifs [5]. Alternative splicing of the single obscurin gene, *OBSCN*, gives rise to giant (720–900 kDa), intermediate (150–500 kDa), and small (<150 kDa) obscurins [6–9]. Earlier work has shown that obscurins are located at the periphery of myofibrillar M-bands and *Z*-discs as well as the cell membrane, where they are appropriately positioned to participate in the integration with other sarcoplasmic elements [5,9,10]. Recently, obscurins were linked to the development of heart failure [11,12]. Accordingly, up-regulation of obscurins was reported in a mouse model of myocardial hypertrophy and a canine model of ventricular tachycardia [13,14], and missense and frameshift mutations in the *OBSCN* gene were linked to the development of cardiomyopathies [11,12,15,16].

While the scaffolding properties of obscurins are well-established [17–19], their functions at the cell membrane are less understood. Herein, we characterize two novel, small obscurin isoforms, obsc-40 and obsc-80, that preferentially localize to the ID of cardiomyocytes. Our studies show that obsc-40 and obsc-80 bind directly to select phosphatidylinositol bisphosphates (PIP2s) via their PH-domain, and negatively regulate the PI3K/AKT/mTOR pathway, therefore contributing to the regulation of cardiomyocyte size and adhesion.

2. Methods

An expanded Methods section is provided in the Supplementary Material online.

2.1. Animal models and tissue collection

Myocardial infarction (MI) and pressure overload (PO) via transverse aortic constriction (TAC) were performed as described [20]. Hypertrophied mice, confirmed by

echocardiography and measurements of heart to bodyweight ratios (Table S1), were euthanized via exsanguination. Hearts were isolated and appropriately stored for further processing (n = 5 for each cohort). In addition, hearts were isolated from wild-type C57BL/6Scsn/J mice (Jackson Laboratories) and Sprague Dawley rats (Harlan, Indianapolis, Indiana) at the indicated ages. All animal procedures were in full compliance with the guidelines approved by the Institutional Animal Care and Use Committee of the University of Maryland School of Medicine and the Ohio State University Wexner Medical Center, and carried out in accordance with the Guide for the Care and Use of Laboratory Animals of the National Institutes of Health.

2.2. Preparation of cultured rat heart myocytes

Rat neonatal cardiac myocytes (RNCM) were isolated from hearts of embryonic day-20 (E20) rats by enzymatic digestion and cultured as reported [21]. Pregnant dams were euthanized via CO_2 asphyxiation followed by cervical dislocation, in accordance with the Guide for the Care and Use of Laboratory Animals of the National Institutes of Health.

2.3. Cell culture and transfections

H9C2 cardiac-derived cells (ATCC, Manassas, VA) were cultured according to the manufacturer's instructions. Twenty-four hours (h) prior to transfection, the cells were switched to differentiation media. Transfections were preformed on RNCM and H9C2 cells using TransIT-2020 Transfection Reagent (Mirus Bio LLC, Madison, WI) per the manufacturer's instructions. DMEM supplemented with 2% FBS was added to the cells 3 h post transfection. Cells were stimulated with insulin for 20 min, 24 h post-transfection.

2.4. Cellular adhesion assay

A cellular adhesion assay was performed as in [22,23] with minor modifications. Transfected RNCM was subjected to dispase proteolysis and orbital rotation to induce fragmentation. The fragments were blindly counted under a dissecting microscope using a 2× objective and the assay was repeated 5 independent times for each condition with three replicates per experiment.

2.5. RNA isolation and reverse transcription-PCR

Total RNA was purified and reverse-transcribed as described [24]. Authenticity of novel obscurin transcripts and amplicons was verified by gel electrophoresis and sequencing; primer sets are listed in Fig. S1 and Table S2.

2.6. Western blotting

Total protein and ID enriched fractions were isolated using previous methods [24,25]. Immunodetection of the indicated proteins was performed as described [24]. To analyze lipids, lysates from H9C2 cells were prepared and dot blots were performed as in [26]. To ensure equal loading, protein concentration for all samples was measured using the Bradford Reagent (Bio-rad Laboratories, Hercules, CA), and 50 μg of protein were prepared for electrophoresis. In addition, membranes were re-probed for GAPDH or HSP90, which served as loading controls, following stripping with the Restore Plus Western Blot Stripping

Buffer (ThermoFisher Scientific), according to the manufacturer's instructions. For the lipid dot blots, HSP90 served as loading control on replica blots. The purity of the ID enriched fractions was verified via staining for N-cadherin, an integral protein of the ID, dystrophin, a membrane protein absent from the ID, and GAPDH, a cytosolic protein [27].

2.7. Immunostaining

Tissue cryosections and cells were stained with primary antibodies recognizing the indicated proteins and imaged as reported [24].

2.8. Immuno-electron microscopy

Perfusion fixed hearts (n = 2) were isolated and the apex, mid and upper regions of the left ventricle were processed for immunoelectron microscopy as described [28]. An n = 20 images per region per heart were evaluated, resulting in analysis of n=120 distinct IDs per antibody.

2.9. Generation of recombinant proteins

Wild-type and mutant forms of the PH-domain of human obscurins (accession #: AJ002535) were produced as GST-fusion proteins, as indicated in [29]; see Table S2 for oligonucleotide sets used for the amplification of the relevant constructs.

2.10. Binding assays

Immunoprecipitation assays were performed using Protein A/G Beads (Life Technologies). Lipid slot blot assays were performed using pre-spotted lipid membrane strips (Echelon Biosciences Inc., Salt Lake City, UT). Membranes were incubated with the indicated recombinant proteins, probed with antibodies recognizing the GST-moiety and processed for immunoblotting as above.

2.11. Computational modeling of the obscurin PH-domain and phospholipid binding

Computational modeling was done using the *C. elegans* PH structure (PDB: 1FHO) as template [30]. PIP derivatives were created and minimized in YASARA. Docked models between the PIP molecules and obscurin-PH domain were subjected to ~10 ns of molecular dynamic (MD) simulation to verify the strength and validity of the PIP-PH interactions.

2.12. Statistical analysis

For the immunoelectron microscopy experiments, the distance of each immuno-gold particle from the center of the ID membrane was measured and presented in a histogram. For histogram analysis, 60 uniform bins were defined for distances between 0 μm and 0.6μm. A bimodal and single Gaussian distribution fit was calculated for distances measured with the α-obscCOOH and α-obscABD antibodies, respectively.

All other results are presented in bar graphs showing Standard Error of the Mean, SEM. Statistical analysis was performed with unpaired 2-tailed *t*-test (for comparisons between two groups; data presented in Figs. 1B and 4I), one-way ANOVA (for comparisons of more than two groups; data presented in Figs. 7A′, B′, C′, Fig. S5A′ and B′), and two-way

ANOVA (for comparisons between more than two groups and more than two variables; data presented in Figs. 5B′, C′, 6A′, B′) with post-hoc Bonferroni correction. P-value <0.05 was considered significant.

3. Results

3.1. Alternative splicing of the OBSCN gene results in the expression of two smaller isoforms

Since the original identification of the human *OBSCN* gene in 2001, the most well-studied obscurin isoforms have been giant obscurins A and B. To date, additional isoforms have been observed mainly via immunoblotting, however their complete molecular architecture is unknown [6,7,9,31]. The recent elucidation of different mammalian and non-mammalian transcriptomes has revealed novel transcripts originating from the single *OBSCN* gene [6]. Using in silico analysis and molecular biology techniques, we identified two novel, small obscurin isoforms, obsc-40 (accession # BC044882) and obsc-80 (accession # BC060226), denoted for their apparent molecular weights (Fig. S1A–E). The presence of transcripts encoding obsc-40 and obsc-80 was confirmed in both mouse and rat adult myocardia by RT-PCR, and is discussed in detail in Supplemental Materials online (Fig. S1F).

To examine the expression profile of small obscurins, we performed immunoblots of protein lysates from adult mouse and rat myocardia, which we probed with antibodies to epitopes along the length of giant obscurins. Specifically, we used α-obscNH$_2$ antibody recognizing epitopes in the first immunoglobulin (Ig) domain of giant obscurins, which are absent from obsc-80 and obsc-40, α-obscCOOH and α-obscRhoGEF/PH antibodies recognizing epitopes in Ig domains 66–67 and the tandem RhoGEF/PH domains, respectively, which are present in obsc-80 and obsc-40 in addition to giant obscurins, and α-obscABD antibody recognizing epitopes in the Ankyrin Binding Domain (ABD) found in obsc-80 and giant obsc-A, but not obsc-40 and giant obsc-B (the epitopes are shown in Fig. 1A). The α-obscCOOH and α-obscRhoGEF/PH antibodies detected two immunoreactive bands that migrated at ~80 and ~40 kDa, corresponding to obsc-80 and obsc-40, while the α-obscABD antibody only detected obsc-80 (Fig. S2A–B). As expected, the α-obscNH$_2$ antibody did not recognize either the ~80 or ~40 kDa bands.

We then interrogated the temporal expression profile of obsc-80 and obsc-40. Both proteins were present in late embryogenesis and throughout postnatal development in mouse myocardium, albeit in varying amounts (Fig. 1B). Interestingly, obsc-80 and obsc-40 exhibited nearly opposite expression patterns during postnatal development. Obsc-80 was the predominant form in mid-embryogenesis (E11), and moderately decreased postnatally and in adulthood, while obsc-40 increased significantly as development progressed (Fig. 1B–B′), while both proteins were expressed in similar amounts during adulthood (Fig. 1B–B′). Notably, the total amount of obsc-80 and obsc-40 remained unchanged throughout development and in maturity (Fig. 1B–B′).

3.2. Novel obscurins-80 and -40 are enriched at the intercalated disc (ID)

Given that the generation of antibodies specific to obsc-80 and obsc-40 is not feasible as they share the same sequence with giant obscurins, we first examined the subcellular localization of exogenous obsc-80 and obsc-40. Overexpression of full-length obsc-80 and obsc-40 conjugated to GFP in primary cultures of RNCM demonstrated that both proteins target to the cell membrane where they co-localize with N-cadherin at cell-cell contacts, with minimal cytosolic accumulation (Fig. 1C–D″). Notably, GFP-alone remained cytosolic and did not co-localize with N-cadherin (Fig. 1E–E″).

To confirm the subcellular distribution of the endogenous small obscurins, we performed subcellular fractionation combined with immunoblotting using the α-obscCOOH antibody. As expected, immunoreactive bands of ~80 and ~40 kDa, corresponding to obsc-80 and obsc-40, were detected in the whole heart (WH) fraction. Consistent with the localization of obsc-80 and obsc-40 in ectopically expressed RNCM, both proteins were enriched in the ID fraction of mouse hearts, compared to the cytosolic (C) and particulate (P) fractions that contained minute (C) or lower (P) amounts (Fig. 1F). The purity of the ID enriched fractions was verified via staining for N-cadherin, an integral protein of the ID, dystrophin, a membrane protein absent from the ID, and GAPDH, a cytosolic protein [27]. Notably, the fractionation patterns of obsc-80 and obsc-40 are nearly identical to that of N-cadherin (Fig. 1F), although minute expression of obsc-80 and obsc-40 in the cytosol and other membrane locations was observed. On the contrary, giant obscurins are enriched in the cytosolic (C) fraction and only detected at very low levels in the ID fraction, confirming previous reports [9], (Fig. 1G).

Using confocal optics along with the panel of obscurin antibodies described above (Fig. 1A), we confirmed the ID localization of endogenous obscurins in cryosections of developing and adult mouse (Fig. 2A–E″) and rat (Fig. S3A–C″) myocardia. Obscurins, stained with the α-obscCOOH and α-obscABD antibodies, were found at the ID and co-localized with other ID proteins (i.e. N-cadherin, desmin, and α-actinin) both during development (Fig. 2A–B″) and at maturity (Fig. 2C–E″ and Fig. S3A–B″); please note that the α-obscCOOH antibody detects both obsc-80 and obsc-40 while the α-obscABD detects only obsc-80. On the contrary, antibodies recognizing the NH_2-terminus of giant obscurins A and B failed to label the ID (Fig. S3C′–C″).

Moreover, our confocal evaluation further demonstrated that obscurins detected with the α-obscCOOH and α-obscABD antibodies localize to distinct regions within the ID during development (i.e. late embryonic and early postnatal stages) and at maturity (i.e. adulthood). During late embryogenesis (i.e. E17) and postnatal development (i.e. P3), obscurins co-distribute with N-cadherin at premature IDs (Fig. 2A–B). However, at maturity, they exhibit two distinct staining patterns (Fig. 2C–E″). Specifically, the α-obscCOOH antibody, detecting both obsc-80 and obsc-40, stains either a doublet that flanks the labeling for N-cadherin or a broad and continuous region that overlaps with and extends beyond the N-cadherin labeling (Fig. 2C and D, respectively, arrow). On the contrary, the α-obscABD antibody, recognizing only obsc-80 at the ID, shows a doublet pattern bordering the N-cadherin staining (Fig. 2E, arrow). Notably, a doublet-staining pattern is also observed for other ID proteins, i.e. desmin (Fig. S3A′, arrow) and α-actinin (Fig. S3B′, arrow). We

quantified the percent occurrence of each staining pattern for all aforementioned proteins, and found that integral ID proteins exhibited a continuous staining pattern, i.e. connexin43 (100%; Fig. S4) and N-cadherin (100%), while peripheral ID proteins displayed a doublet-staining pattern, i.e. desmin (100%) and α-actinin (100%). Interestingly, the α-obscABD antibody, detecting obsc-80, solely labeled a doublet (100%), whereas the α-obscCOOH antibody, recognizing both obsc-80 and obsc-40, stained a doublet (65%) and a continuous band (35%). Thus, during development obsc-80 and obsc-40 co-distribute at the ID, however in adulthood they likely localize to distinct regions.

To further interrogate the differential distribution of obsc-80 and obsc-40 in the ID of adult myocardia, we employed immunoelectron microscopy, and calculated the distance of each gold particle from the center of the space between two adjoining cardiomyocytes. The α-obscCOOH antibody labeled the entire ID, concentrating at the peaks of the ID folds (Fig. 2F, red arrows) and the surrounding electrondense area (Fig. 2F, green arrows). Interestingly, the distribution of the measured distances yielded two distinct populations, averaging ~0.02 μm and ~0.5 μm from the center of the ID space between cardiomyocytes (Fig. 2H, the two populations are noted in green). On the contrary, the α-obscABD antibody associated predominantly with the peaks of the ID folds (Fig. 2G, red arrows), and the measured distances yielded a single population with an average distance of ~0.02 μm from the center of the space between neighboring cells (Fig. 2H, red population).

Given small obscurins' distinct localizations in the ID, we next examined whether they preferentially associate with different ID proteins. To address this, we performed co-immunoprecipitation assays using protein lysates prepared from adult mouse hearts and a panel of antibodies to major ID proteins (Fig. 3). Both obsc-80 and obsc-40were detected in immunoprecipitates generated with antibodies to desmosomal (Fig. 3A–B, α-desmoglein-2 and α-desmin), gap junction (Fig. 3C, α-connexin43), and adherens junction (Fig. 3D, α-N-cadherin) proteins. Notably, obsc-80 was also detected in immunoprecipitates generated with antibodies to ankyrinG and vinculin (Fig. 3E–F), which also localize to the peaks of the folds of the ID membrane [4,32]. In contrast, obsc-40 was only present in minute amounts in the ankyrinG- and vinculin-generated immunoprecipitate fractions (Fig. 3E–F). Collectively, our immunological and biochemical data support that small obscurins -80 and -40 concentrate in two distinct regions at the ID, where they (directly or indirectly) interact with other prominent ID proteins.

3.3. The obscurin PH-domain interacts with select phosphatidyl-inositol bisphosphates

Previous literature supports the regulatory role of PH domains through their phospholipid binding capacities [33]. We therefore investigated the ability of the obscurin-PH domain to interact with distinct phosphatidyl-inositol phosphates (PIPs). To this end, we used pre-spotted lipid membranes and assessed their binding to recombinant GST-obscurin-PH protein in in vitro binding assays. The obscurin-PH domain bound strongly to phosphatidyl-inositol (3,4) and (4,5) bisphosphates (PIP2s) and to a lesser extent to single phosphatidyl-inositol (3), (4) or (5) phosphate and triple phosphatidyl-inositol (3,4,5) phosphate (Fig. 4A). The observed binding was specific to the obscurin-PH domain since control GST-protein failed to show any binding (Fig. 4B).

To identify the lipid-binding pocket of the obscurin-PH domain, we used computational modeling along with site directed mutagenesis and in vitro binding assays. We modeled the molecular structure of the human obscurin PH-domain using the solution structure of the UNC-89 PH-domain, the *C. elegans* homologue of mammalian obscurin (PDB: 1FHO) [30,34,35]; the two domains share 48% homology. Similar to canonical PH-domains, the human obscurin PH-domain folds into a 7-stranded β-sandwich structure (Fig. 4C) [33,36]. Canonical PH-domains confer PI binding, which is often mediated by the sequence motif "KX_nK/RY_nR", where X can be Pro, Gly, Ala or Ser, and Y can be any amino-acid [36], with the basic side chains from the K and R residues forming electrostatic interactions with the phosphate headgroups. The obscurin PH-domain contains two possible lipid-binding sites (PLBS). PLBS 1 possesses the canonical KPRRDSR signature motif (Fig. 4C, highlighted in red), whereas PLBS 2 contains a non-canonical lipid binding sequence, REDSVRK; both maintain the essential basic side chains necessary for PIP binding (Fig. 4C, highlighted in green). Both PLBS are 100% homologous between the human and mouse sequences (Fig. 4D). However, the basic side chains within PLBS 1 and 2 are not conserved in the UNC-89 PH-domain sequence.

Using alanine-scanning mutagenesis, we mutated two positively charged residues in PLBS 1 (R40 and R41) and PLBS 2 (R80 and R85) and assayed them for their ability to interact with $PI(3,4)P_2$ and $PI(4,5)P_2$ using pre-spotted lipid membranes. The PLBS 1 mutations did not change the binding capacity of the obscurin PH-domain for $PI(3,4)P_2$ or $PI(4,5)P_2$ (Fig. 4E&I). However, elimination of the positively charged residues within PLBS 2 resulted in an ~5-fold decrease in the binding capacity of the obscurin PH-domain for $PI(3,4)P_2$ and $PI(4,5)P_2$, suggesting that PLBS 2 mediates binding to the indicated PIP2s (Fig. 4F&I). Single alanine mutants of R80 and R85 showed a 2-fold decrease in PI(4,5)P2 binding and a 3-fold decrease in PI(3,4)P2 binding, respectively (Fig. 4G–I). In contrast, there was no significant loss of binding between R80 and $PI(3,4)P_2$ or R85 and $PI(4,5)P_2$ (Fig. 4G–I).

In parallel to our in vitro binding assays, we simulated the dynamic molecular interaction between the obscurin PH-domain and $PI(3,4)P_2$ or $PI(4,5)P_2$ to identify the electrostatic interactions that mediate their binding. Molecular dynamic simulations and homology modeling suggested that R80 and R85 comprise a small positively charged pocket on the exterior of the obscurin PH-domain. Furthermore, docking algorithms with subsequent molecular dynamic simulations indicated the presence of electrostatic interactions between both positively charged side chains of R80 and R85 in PLBS 2 and the negatively charged headgroup of $PI(3,4)P_2$ (Fig. 4J), and between the positively charged side chain of R80 and the negatively charged headgroup of $PI(4,5)P_2$ (Fig. 4K). In support of our biochemical data, models that docked either $PI(3,4)P_2$ or $PI(4,5)P_2$ near PLBS 1 demonstrated no appreciable binding. Together, our biochemical and dynamic molecular modeling findings support a model in which R85 and R80 are necessary for binding to $PI(3,4)P_2$ and $PI(4,5)P_2$, respectively, and that their binding is mediated by electrostatic interactions.

3.4. Small obscurins regulate the PI3K/AKT/mTOR signaling pathway through their PH-domain

It is well documented that PI3K controls the balance between PIP2s and phosphatidylinositol trisphosphate (PIP3) at the membrane, which in turn regulates the PI3K/AKT/mTOR pathway [37]. We therefore examined the effects of the obscurin PH-domain on the ratio of PIP2:PIP3 and the activation of the PI3K/AKT/mTOR pathway. To do so, we used the H9C2 cardiac-derived cells, an established cell model for studying myocyte signaling and hypertrophy [38–41] to transfect GFP-tagged obscurin PH-domain, GFP-obsc-40, GFP-obsc-80 or control GFP-alone (Fig. 5A). First, we assessed the relative levels of PIP2s and PIP3 by dot-blot assay. Control cells expressing GFP-protein contained equivalent amounts of PIP2 and PIP3 in the absence of insulin; however, upon insulin stimulation PIP3 levels were significantly increased compared to PIP2 levels (Fig. 5B–B′). On the contrary, overexpression of the obscurin PH-domain, obsc-40 or obsc-80 resulted in a clear shift of the relative levels of PIP2s and PIP3 toward PIP2s upon insulin stimulation (Fig. 5B–B′).

Given the shift in the ratio of endogenous PIP2:PIP3 toward PIP2s in cardiomyocytes overexpressing the PH-domain, obsc-40 or obsc-80 we next assessed the activation state of key components of the PI3K/AKT/mTOR pathway by assaying for their phosphorylation levels in the absence or presence of insulin. Immunoblotting revealed a significant decrease in the levels of the phosphorylated forms of major components of the PI3K/AKT/mTOR pathway (Fig. 5C–C′). Specifically, we detected a considerable decrease in the phosphorylation levels of PI3K at Y458, a phospho-site correlated with the activation levels of the enzyme [42], AKT at T308 and S473 indicating its reduced activation, and mechanistic target of rapamycin, mTOR, at S2448 leading to its inactivation [43,44].

Activation of the PI3K/AKT/mTOR pathway in cardiomyocytes results in increased cellular adhesion and growth [45,46]. We therefore first investigated the role of small obscurins in cardiac adhesion. Primary RNCM overexpressing the obscurin PH-domain, obsc-40 or obsc-80 were plated to confluence, enzymatically released from the dish, and subjected to mechanical stress via orbital rotation to induce fragmentation of the monolayer. Overexpression of the obscurin PH-domain, obsc-40 or obsc-80 drastically reduced myocyte adhesion as shown by the increased fragmentation of the cell monolayer compared to control GFP-protein (Fig. 6A–A′); insulin treatment, however, did not significantly exacerbate their effects.

Next, we interrogated the role of small obscurins in modulating cell size (Fig. 6B–B′). Phase contrast images of transiently transfected RNCM were used to measure cellular area at their optical midsection, as determined by confocal imaging of α-actinin staining. RNCM overexpressing the obscurin PH-domain or either of the small obscurins exhibited significantly reduced size compared to control cells expressing GFP-alone (Fig. 6B); notably, this effect was observed in the absence and presence of insulin.

Taken together, our data suggest that through its interaction with select PIP2s the obscurin PH-domain may act as a “sink” for PIP2s, limiting their availability and phosphorylation by

PI3K, thus precluding the activation of the PI3K/AKT/mTOR pathway, which in turn results in reduced cell adhesion and growth.

3.5. Small obscurins' expression is increased in acute and chronic animals models of heart failure

In accordance with the documented role of over-activated PI3K/AKT/mTOR cascade in heart failure patients [47,48] as well as the emerging role of mutant obscurins in the development of cardiomyopathies [11,12,15], [16], we investigated the protein and mRNA levels of obsc-80 and obsc-40 in acute (i.e. myocardial infarction, MI) and chronic (i.e. pressure overload, PO) cardiac-stress mouse models (Fig. 7). Immunoblotting using the α-obscCOOH antibody revealed that the protein levels of both obsc-80 and obsc-40 were significantly decreased in both cardiac-stress models compared to sham controls (Fig. 7A–A′). On the contrary, the levels of giant obscurins A and B remained unchanged compared to control (Fig. 7A–A′). The altered levels of the small obscurin isoforms in the MI and PO models are likely due to changes in protein turnover, since their transcript levels are unaltered compared to control (Fig. S5A–A′). In addition, the levels of other ID proteins, including N-cadherin, connexin43, desmoglein-2, and vinculin exhibited no change (Fig. S6A–A′). Interestingly, however, the protein levels of ankyrinG, found in a complex with obsc-80, but not obsc-40 (Fig. 3E), were also decreased relative to control (Fig. S6A–A′).

Consistent with the reduced activation of the PI3K/AKT/mTOR pathway following overexpression of either the obscurin PH-domain, obsc-40 or obsc-80 (Fig. 4), key components of the PI3K/AKT/mTOR pathway were hyper-phosphorylated (and thus over-activated) in the MI and PO cardiac-stress models compared to control (Fig. 7B–B′). Along with these molecular alterations, we also observed a shift in the ratio of PIP2s:PIP3 toward PIP3 in both the MI and PO models compared to control (Fig. 7C–C′). Thus, decreased levels of obsc-80 and obsc-40, as seen in the acute MI and chronic PO cardiac-stress models, result in accumulation of PIP3s and enhanced activation of the PI3K/AKT/mTOR pathway.

4. Discussion

Over the last fifteen years the roles of obscurins have been systematically studied in striated muscles and more recently in breast epithelium [49]. These studies demonstrate that obscurins reside in distinct subcellular compartments, and their localization dictates their specialized functions.

In the current study, we provide the first molecular and functional characterization of two novel smaller obscurin isoforms, obsc-80 and obsc-40. Both isoforms are expressed in the myocardium and preferentially localize to the ID. Obsc-80 and obsc-40 transcripts result from complex alternative splicing at the 3′ end of the *OBSCN* gene. Obsc-80 contains the obscurin PH-domain, two Ig domains, corresponding to Ig66 and Ig67 of giant obsc-A and obsc-B, and the ~400-amino acid long COOH-terminus of obsc-A. Obsc-40 is also composed of the obscurin PH-domain and the same Ig domains, but contains a short COOH-terminus consisting of 7 novel residues, which are absent from obsc-A, obsc-B and obsc-80. Through their PH-domain, obsc-80 and obsc-40 interact with PIP2s, precluding their conversion to PIP3, thereby antagonizing the PI3K/AKT/mTOR pathway and fine-tuning

cardiomyocyte size and adhesion (Fig. 8). In agreement with this, the protein levels of obsc-80 and obsc-40 are reduced in acute and chronic models of cardiac stress. Thus, our studies are not only the first to identify and characterize two novel obscurin isoforms, but also to implicate obscurins in heart disease via the regulation of the PI3K/AKT/mTOR pathway.

Previous work has alluded to the presence of smaller obscurin isoforms, however their molecular and functional characterization is still lacking [6–9]. Using immunoblot analysis, we have shown that several smaller obscurins are expressed in mammalian striated muscle and non-muscle tissues [6]. In the heart, there are at least fifteen immunoreactive bands that contain epitopes present along giant obscurins. Although technical issues have precluded the identification of lower molecular weight isoforms, such as obsc-40, our studies consistently identified an immunoreactive band of ~80 kDa in multiple mammalian tissues, including skeletal and cardiacmuscles, brain, kidney, liver, lung, spleen, and skin [6]. In addition, an ~80 kDa immunoreactive band has been detected in breast (MCF10A) and colon (FHC) epithelial cell lines [31]. These findings along with our previous observations demonstrating the presence of obscurins at cell junctions in epithelial cells and hepatocytes [6,31] suggest that obsc-80 is ubiquitously expressed among mammalian tissues and organs, where it preferentially localizes at cell junctions potentially regulating the PI3K/AKT/mTOR cascade.

Studying the subcellular localization of obsc-80 and obsc-40 presents unique challenges, as the amino acid composition of both small isoforms is nearly identical to giant obsc-A, and therefore it is not possible to generate isoform-specific antibodies. Thus, we devised a method that is based on combinatorial epitopemapping for our immunoblot assays and subcellular localization studies (Fig. 2, Figs. S2 & S3). Using a panel of antibodies to epitopes present in both obsc-80 and obsc-40 (α-obscCOOH and α-obscRhoGEF/PH), selective for obsc-80 and giant obsc-A (α-obscABD), and absent from both obsc-80 and obsc-40 but recognizing giant obsc-A and obsc-B (α-obscNH_2), we were able to study the expression pattern and subcellular distribution of obsc-80 and obsc-40 in the heart. Obsc-80 and obsc-40 preferentially localize to the ID, however their subcellular distribution at the ID is unique for each isoform.

Obsc-80 is abundantly expressed early in the developing heart, persists throughout maturity, and concentrates at the peaks of the folds of the ID membrane. Obsc-40 is not expressed until postnatal development, and localizes throughout the ID membrane. While the ratio of obsc-80 and obsc-40 varies during development and at maturity, the total amount of the proteins remains unaltered. Although the two small obscurins share the same NH_2-termini, their COOH-termini are distinct. Specifically, obsc-80 contains an ABD and several potential ERK kinase phosphorylation sites, which are absent fromobsc-40. Thus, obsc-80 may preferentially interact with ankyrins that also localize to the ID (Fig. 3), and may be regulated via ERK-mediated phosphorylation. Conversely, obsc-40 contains seven novel amino acid residues (-ERRPSPP) at its extreme COOH-terminus, which are highly charged, while the serine is predicted to be phosphorylated. Although the functional significance of the unique COOH-terminus of obsc-40 is currently elusive, it is tempting to speculate that it may contribute to its targeting, binding interactions, or regulation.

The ability of obsc-80 and obsc-40 to regulate the PI3K/AKT/mTOR pathway comes from their capacity to bind select PIP2s through their PH-domain. PIP2s are short-lived secondary messengers, functioning to recruit signaling proteins that contain PIP-binding motifs (e.g. PH-domains) to the cell membrane [33]. Upon stimulation with growth factors, PI3K is activated and phosphorylates PIP2s, generating PIP3, which acts as an adaptor to recruit the downstream effectors PDK1 and AKT to the cell membrane [50]. Membrane localization of AKT results in its activation via phosphorylation at T308 and S473 by PDK1 [50]. mTOR, a downstream target of AKT, plays major roles in cardiac (patho) physiology [51]. Among its many functions, mTOR mediates cardiac adaptation to chronic stress by contributing to the development of compensatory hypertrophy through its ability to regulate cardiomyocyte growth and adhesion [52,53]. Inhibition of the mTOR pathway reduces pathological hypertrophy and heart failure [54,55]. Cardiomyocytes overexpressing obsc-80, obsc-40 or the PH-domain exhibited reduced levels of active PI3K/AKT/mTOR, and were considerably smaller in size and less likely to form stable adhesion junctions. Consistent with these observations, hypertrophied hearts subjected to acute (MI) and chronic (PO) stressors contained markedly decreased amounts of obsc-80 and obsc-40, a lower ratio of PIP2s:PIP3, and significantly increased levels of active PI3K/AKT/mTOR. This reciprocal relationship between the activation of the PI3K/AKT/mTOR pathway and the expression levels of obsc-80 and obsc-40 indicates that small obscurins may act as negative regulators of the PI3K/AKT/mTOR cascade, thus contributing to the fine-tuning of cardiomyocyte size and adhesion (Fig. 8).

Vinculin, an ID protein that is in a complex with obsc-80, also interacts with PIP2s, and functions as a sensor to modulate how phospholipids regulate cellular adhesion [56,57]. Down-regulation of vinculin in cardiomyocytes results in significantly reduced phosphorylation (and thus diminished activation) of the PI3K/AKT/mTOR cascade [58]. As regulation of cell adhesion and size are of paramount importance, it is reasonable to assume that cardiomyocytes have devised numerous mechanisms to modulate these processes. It is therefore possible that vinculin and obsc-80, which exist in a complex, act antagonistically to regulate the PI3K/AKT/mTOR pathway and thus cardiomyocyte adhesion and size.

Taken together, our studies demonstrate the preferential localization of two novel, small obscurin isoforms to the ID. Through their PH domain these novel obscurin isoforms modulate the activation of the PI3K/AKT/mTOR cascade, potentially by competing with PI3K for binding to PIP2s. Future studies will examine this possibility, and further assess the involvement of small obscurins -80 and -40 in the pathogenesis of idiopathic and congenital heart disease.

Supplementary Material

Refer to Web version on PubMed Central for supplementary material.

Acknowledgments

Funding

This work was supported by grants from National Institutes of Health (HL116778 to M.A.A.); Research Corporation Cottrell College (22450 to N.T.W.); National Science Foundation (CHE-1461175 to N.T.W.); and American Heart Association (14GRNT20380360 & 16GRNT31290010 to A.K.K.).

The authors would like to thank the late Dr. William Stanley for his mentorship and technical support.

References

1. Calore M, Lorenzon A, De Bortoli M, Poloni G, Rampazzo A. Arrhythmogenic cardiomyopathy: a disease of intercalated discs. Cell Tissue Res. 2015; 360:491–500. [PubMed: 25344329]
2. Li J, Radice GL. A new perspective on intercalated disc organization: implications for heart disease. Dermatol. Res. Pract. 2010; 2010:207835. [PubMed: 20585598]
3. Delmar M. The intercalated disk as a single functional unit. Heart Rhythm. 2004; 1:12–13. [PubMed: 15851109]
4. Bennett PM, Maggs AM, Baines AJ, Pinder JC. The transitional junction: a new functional subcellular domain at the intercalated disc. Mol. Biol. Cell. 2006; 17:2091–2100. [PubMed: 16481394]
5. Kontrogianni-Konstantopoulos A, Ackermann MA, Bowman AL, Yap SV, Bloch RJ. Muscle giants: molecular scaffolds in sarcomerogenesis. Physiol. Rev. 2009; 89:1217–1267. [PubMed: 19789381]
6. Ackermann MA, Shriver M, Perry NA, Hu LY, Kontrogianni-Konstantopoulos A. Obscurins: goliaths and davids take over non-muscle tissues. PLoS One. 2014; 9:e88162. [PubMed: 24516603]
7. Fukuzawa A, Idowu S, Gautel M. Complete human gene structure of obscurin: implications for isoform generation by differential splicing. J. Muscle Res. Cell Motil. 2005; 26:427–434. [PubMed: 16625316]
8. Russell MW, Raeker MO, Korytkowski KA, Sonneman KJ. Identification, tissue expression and chromosomal localization of human obscurin-MLCK, a member of the titin and Dbl families of myosin light chain kinases. Gene. 2002; 282:237–246. [PubMed: 11814696]
9. Hu LY, Kontrogianni-Konstantopoulos A. The kinase domains of obscurin interact with intercellular adhesion proteins. FASEB J. 2013; 27:2001–2012. [PubMed: 23392350]
10. Spooner PM, Bonner J, Maricq AV, Benian GM, Norman KR. Large isoforms of UNC-89 (obscurin) are required for muscle cell architecture and optimal calcium release in *Caenorhabditis elegans*. PLoS One. 2012; 7:e40182. [PubMed: 22768340]
11. Arimura T, Matsumoto Y, Okazaki O, Hayashi T, Takahashi M, Inagaki N, et al. Structural analysis of obscurin gene in hypertrophic cardiomyopathy. Biochem. Biophys. Res. Commun. 2007; 362:281–287. [PubMed: 17716621]
12. Marston S, Montgiraud C, Munster AB, Copeland O, Choi O, Dos Remedios C, et al. OBSCN mutations associated with dilated cardiomyopathy and haploinsufficiency. PLoS One. 2015; 10:e0138568. [PubMed: 26406308]
13. Borisov AB, Raeker MO, Kontrogianni-Konstantopoulos A, Yang K, Kurnit DM, Bloch RJ, et al. Rapid response of cardiac obscurin gene cluster to aortic stenosis: differential activation of Rho-GEF and MLCK and involvement in hypertrophic growth. Biochem. Biophys. Res. Commun. 2003; 310:910–918. [PubMed: 14550291]
14. Borisov AB, Sutter SB, Kontrogianni-Konstantopoulos A, Bloch RJ, Westfall MV, Russell MW. Essential role of obscurin in cardiac myofibrillogenesis and hypertrophic response: evidence from small interfering RNA-mediated gene silencing. Histochem. Cell Biol. 2006; 125:227–238. [PubMed: 16205939]
15. Xu J, Li Z, Ren X, Dong M, Li J, Shi X, et al. Investigation of pathogenic genes in Chinese sporadic hypertrophic cardiomyopathy patients by whole exome sequencing. Sci Rep. 2015; 5:16609. [PubMed: 26573135]
16. Rowland TJ, Graw SL, Sweet ME, Gigli M, Taylor MR, Mestroni L. Obscurin variants in patients with left ventricular noncompaction. J. Am. Coll. Cardiol. 2016; 68:2237–2238. [PubMed: 27855815]
17. Kontrogianni-Konstantopoulos A, Catino DH, Strong JC, Sutter S, Borisov AB, Pumplin DW, et al. Obscurin modulates the assembly and organization of sarcomeres and the sarcoplasmic reticulum. FASEB J. 2006; 20:2102–2111. [PubMed: 17012262]

18. Kontrogianni-Konstantopoulos A, Jones EM, Van Rossum DB, Bloch RJ. Obscurin is a ligand for small ankyrin 1 in skeletal muscle. Mol. Biol. Cell. 2003; 14:1138–1148. [PubMed: 12631729]
19. Lange S, Ouyang K, Meyer G, Cui L, Cheng H, Lieber RL, et al. Obscurin determines the architecture of the longitudinal sarcoplasmic reticulum. J. Cell Sci. 2009; 122:2640–2650. [PubMed: 19584095]
20. Hecker PA, Lionetti V, Ribeiro RF Jr, Rastogi S, Brown BH, O'Connell KA, et al. Glucose 6-phosphate dehydrogenase deficiency increases redox stress and moderately accelerates the development of heart failure. Circ. Heart Fail. 2013; 6:118–126. [PubMed: 23170010]
21. Rogers TB, Gaa ST, Allen IS. Identification and characterization of functional angiotensin II receptors on cultured heart myocytes. J. Pharmacol. Exp. Ther. 1986; 236:438–444. [PubMed: 3003343]
22. Hariharan V, Asimaki A, Michaelson JE, Plovie E, MacRae CA, Saffitz JE, et al. Arrhythmogenic right ventricular cardiomyopathy mutations alter shear response without changes in cell-cell adhesion. Cardiovasc. Res. 2014; 104:280–289. [PubMed: 25253076]
23. Hobbs RP, Amargo EV, Somasundaram A, Simpson CL, Prakriya M, Denning MF, et al. The calcium ATPase SERCA2 regulates desmoplakin dynamics and intercellular adhesive strength through modulation of PKC & alpha; signaling. FASEB J. 2011; 25:990–1001. [PubMed: 21156808]
24. Ackermann MA, Hu LY, Bowman AL, Bloch RJ. Kontrogianni-Konstantopoulos A. Obscurin interacts with a novel isoform of MyBP-C slow at the periphery of the sarcomeric M-band and regulates thick filament assembly. Mol. Biol. Cell. 2009; 20:2963–2978. [PubMed: 19403693]
25. Kargacin GJ, Hunt D, Emmett T, Rokolya A, McMartin GA, Wirch E, et al. Localization of telokin at the intercalated discs of cardiac myocytes. Arch. Biochem. Biophys. 2006; 456:151–160. [PubMed: 16884679]
26. Li J, Russell B. Phosphatidylinositol 4,5-bisphosphate regulates CapZbeta1 and actin dynamics in response to mechanical strain. Am. J. Physiol. Heart Circ. Physiol. 2013; 305:H1614–23. [PubMed: 24043251]
27. Petitprez S, Zmoos AF, Ogrodnik J, Balse E, Raad N, El-Haou S, et al. SAP97 and dystrophin macromolecular complexes determine two pools of cardiac sodium channels Nav1.5 in cardiomyocytes. Circ. Res. 2011; 108:294–304. [PubMed: 21164104]
28. Kontrogianni-Konstantopoulos A, Bloch RJ. Obscurin: a multitasking muscle giant. J. Muscle Res. Cell Motil. 2005; 26:419–426. [PubMed: 16625317]
29. Borzok MA, Catino DH, Nicholson JD, Kontrogianni-Konstantopoulos A, Bloch RJ. Mapping the binding site on small ankyrin 1 for obscurin. J. Biol. Chem. 2007; 282:32384–32396. [PubMed: 17720975]
30. Blomberg N, Baraldi E, Sattler M, Saraste M, Nilges M. Structure of a PH domain from the *C elegans* muscle protein UNC-89 suggests a novel function. Structure. 2000; 8:1079–1087. [PubMed: 11080629]
31. Perry NA, Shriver M, Mameza MG, Grabias B, Balzer E, Kontrogianni-Konstantopoulos A. Loss of giant obscurins promotes breast epithelial cell survival through apoptotic resistance. FASEB J. 2012; 26:2764–2775. [PubMed: 22441987]
32. Lowe JS, Palygin O, Bhasin N, Hund TJ, Boyden PA, Shibata E, et al. Voltage-gated Nav channel targeting in the heart requires an ankyrin-G dependent cellular pathway. J. Cell Biol. 2008; 180:173–186. [PubMed: 18180363]
33. Lemmon MA. Pleckstrin homology (PH) domains and phosphoinositides. Biochem. Soc. Symp. 2007:81–93. [PubMed: 17233582]
34. Benian GM, Tinley TL, Tang X, Borodovsky M. The *Caenorhabditis elegans* gene unc-89, required fpr muscle M-line assembly, encodes a giant modular protein composed of Ig and signal transduction domains. J. Cell Biol. 1996; 132:835–848. [PubMed: 8603916]
35. Qadota H, McGaha LA, Mercer KB, Stark TJ, Ferrara TM, Benian GM. A novel protein phosphatase is a binding partner for the protein kinase domains of UNC-89 (Obscurin) in Caenorhabditis Elegans. Mol. Biol. Cell. 2008; 19:2424–2432. [PubMed: 18337465]
36. Lemmon MA. Membrane recognition by phospholipid-binding domains. Nat. Rev. Mol. Cell Biol. 2008; 9:99–111. [PubMed: 18216767]

37. Sussman MA, Volkers M, Fischer K, Bailey B, Cottage CT, Din S, et al. Myocardial AKT: the omnipresent nexus. Physiol. Rev. 2011; 91:1023–1070. [PubMed: 21742795]
38. Gurusamy N, Lekli I, Mukherjee S, Ray D, Ahsan MK, Gherghiceanu M, et al. Cardioprotection by resveratrol: a novel mechanism via autophagy involving the mTORC2 pathway. Cardiovasc. Res. 2010; 86:103–112. [PubMed: 19959541]
39. Hescheler J, Meyer R, Plant S, Krautwurst D, Rosenthal W, Schultz G. Morphological, biochemical, and electrophysiological characterization of a clonal cell (H9c2) line from rat heart. Circ. Res. 1991; 69:1476–1486. [PubMed: 1683272]
40. Kimes BW, Brandt BL. Properties of a clonal muscle cell line from rat heart. Exp. Cell Res. 1976; 98:367–381. [PubMed: 943302]
41. Watkins SJ, Borthwick GM, Arthur HM. The H9C2 cell line and primary neonatal cardiomyocyte cells show similar hypertrophic responses in vitro. In Vitro Cell Dev. Biol. Anim. 2011; 47:125–131. [PubMed: 21082279]
42. Rush J, Moritz A, Lee KA, Guo A, Goss VL, Spek EJ, et al. Immunoaffinity profiling of tyrosine phosphorylation in cancer cells. Nat. Biotechnol. 2005; 23:94–101. [PubMed: 15592455]
43. Chiang GG, Abraham RT. Phosphorylation of mammalian target of rapamycin (mTOR) at Ser-2448 is mediated by p70S6 kinase. J. Biol. Chem. 2005; 280:25485–25490. [PubMed: 15899889]
44. Warfel NA, Niederst M, Newton AC. Disruption of the interface between the pleckstrin homology (PH) and kinase domains of Akt protein is sufficient for hydrophobic motif site phosphorylation in the absence of mTORC2. J. Biol. Chem. 2011; 286:39122–39129. [PubMed: 21908613]
45. Laplante M, Sabatini DM. mTOR signaling at a glance. J. Cell Sci. 2009; 122:3589–3594. [PubMed: 19812304]
46. Maillet M, van Berlo JH, Molkentin JD. Molecular basis of physiological heart growth: fundamental concepts and new players. Nat. Rev. Mol. Cell Biol. 2013; 14:38–48. [PubMed: 23258295]
47. Chaanine AH, Hajjar RJ. AKT signalling in the failing heart. Eur. J. Heart Fail. 2011; 13:825–829. [PubMed: 21724622]
48. Walsh K. Akt signaling and growth of the heart. Circulation. 2006; 113:2032–2034. [PubMed: 16651482]
49. Perry NA, Ackermann MA, Shriver M, Hu LY, Kontrogianni-Konstantopoulos A. Obscurins: unassuming giants enter the spotlight. IUBMB Life. 2013; 65:479–486. [PubMed: 23512348]
50. Hemmings BA, Restuccia DF. PI3K-PKB/Akt pathway. Cold Spring Harb. Perspect. Biol. 2012; 4:a011189. [PubMed: 22952397]
51. Sciarretta S, Volpe M, Sadoshima J. Mammalian target of rapamycin signaling in cardiac physiology and disease. Circ. Res. 2014; 114:549–564. [PubMed: 24481845]
52. Shende P, Plaisance I, Morandi C, Pellieux C, Berthonneche C, Zorzato F, et al. Cardiac raptor ablation impairs adaptive hypertrophy, alters metabolic gene expression, and causes heart failure in mice. Circulation. 2011; 123:1073–1082. [PubMed: 21357822]
53. Zhang D, Contu R, Latronico MV, Zhang J, Rizzi R, Catalucci D, et al. MTORC1 regulates cardiac function and myocyte survival through 4E-BP1 inhibition in mice. J. Clin. Invest. 2010; 120:2805–2816. [PubMed: 20644257]
54. McMullen JR, Sherwood MC, Tarnavski O, Zhang L, Dorfman AL, Shioi T, et al. Inhibition of mTOR signaling with rapamycin regresses established cardiac hypertrophy induced by pressure overload. Circulation. 2004; 109:3050–3055. [PubMed: 15184287]
55. Shioi T, McMullen JR, Tarnavski O, Converso K, Sherwood MC, Manning WJ, et al. Rapamycin attenuates load-induced cardiac hypertrophy in mice. Circulation. 2003; 107:1664–1670. [PubMed: 12668503]
56. Chandrasekar I, Stradal TE, Holt MR, Entschladen F, Jockusch BM, Ziegler WH. Vinculin acts as a sensor in lipid regulation of adhesion-site turnover. J. Cell Sci. 2005; 118:1461–1472. [PubMed: 15769850]
57. Palmer SM, Playford MP, Craig SW, Schaller MD, Campbell SL. Lipid binding to the tail domain of vinculin: specificity and the role of the N and C termini. J. Biol. Chem. 2009; 284:7223–7231. [PubMed: 19110481]

58. Zemljic-Harpf AE, Godoy JC, Platoshyn O, Asfaw EK, Busija AR, Domenighetti AA, et al. Vinculin directly binds zonula occludens-1 and is essential for stabilizing connexin-43-containing gap junctions in cardiac myocytes. J. Cell Sci. 2014; 127:1104–1116. [PubMed: 24413171]

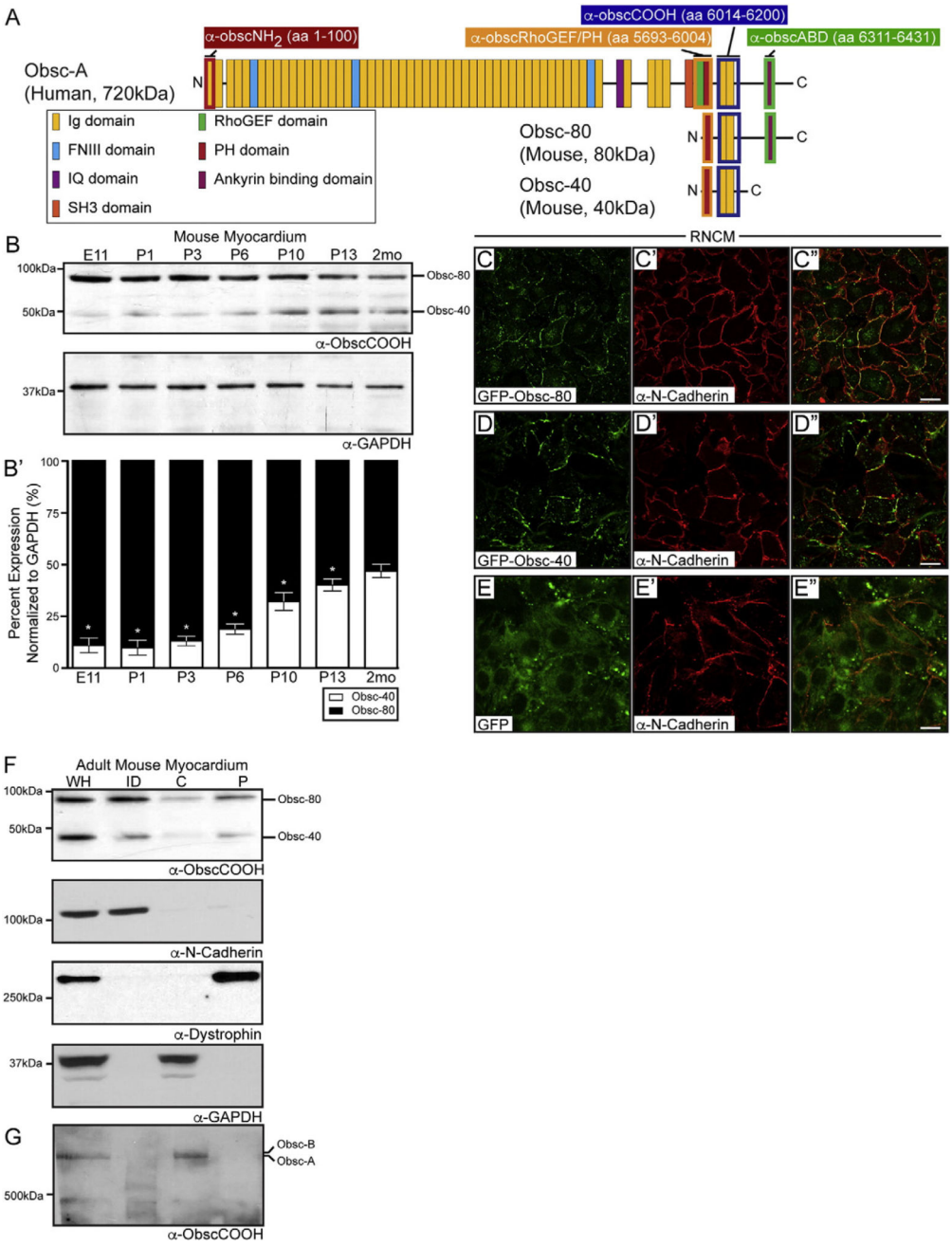

Fig. 1.

Small obscurins are expressed in developing and mature hearts, localize at cardiomyocyte junctions, and are enriched in the ID fraction. (A) Domain architecture of canonical obscurin (obsc-A) and two novel variants (obsc-80 and obsc-40) illustrating their structural and signaling motifs. The epitopes for the obscurin antibodies used in this study are highlighted; please see key for notations. (B) Immunoblots of protein lysates prepared from developing and adult mouse hearts were stained for obscurins with the α-ObscCOOH antibody. GAPDH antibody staining of the same blot following stripping indicates equal loading of lysates. (B′) Quantification of the relative expression levels of obsc-80 and obsc-40 in

developing and adult mouse myocardia (n = 5 hearts per age); the expression of obsc-80 and obsc-40 was normalized to that of GAPDH. The levels of obsc-80 plus obsc-40 in developing cardiac tissue were calculated as a percentage of the total amount in mature tissue, which was set at 100%. Although obsc-80 and obsc-40 are expressed in varying amounts throughout development and at maturity, their total levels remained unaltered. Student's *t*-test was performed to determine significance between the levels of obsc-80 and obsc-40 at different ages, $p < 0.05$. (C–E″) Transiently expressed GFP-obsc-80 (C) and GFP-obsc-40 (D), but not control GFP-protein (E), co-localize with N-cadherin (C′, D′, and E′; staining in red) at cell-cell junctions in primary RNCM. Scale bar 20 μm. (F–G) Subcellular fractionation of adult mouse whole heart (WH) lysates probed with α-ObscCOOH antibody for obsc-80 (F), obsc-40 (F), and giant obscurins (G). Results indicate that obsc-80 and obsc-40 are enriched in the ID fraction, compared to the cytosolic (C) and particulate (P) fractions; and giant obscurins are enriched in the cytosolic (C) fraction. N-cadherin, dystrophin, and GAPDH (F) were used as loading and purity controls for the ID, particulate, and cytosolic fractions, respectively.

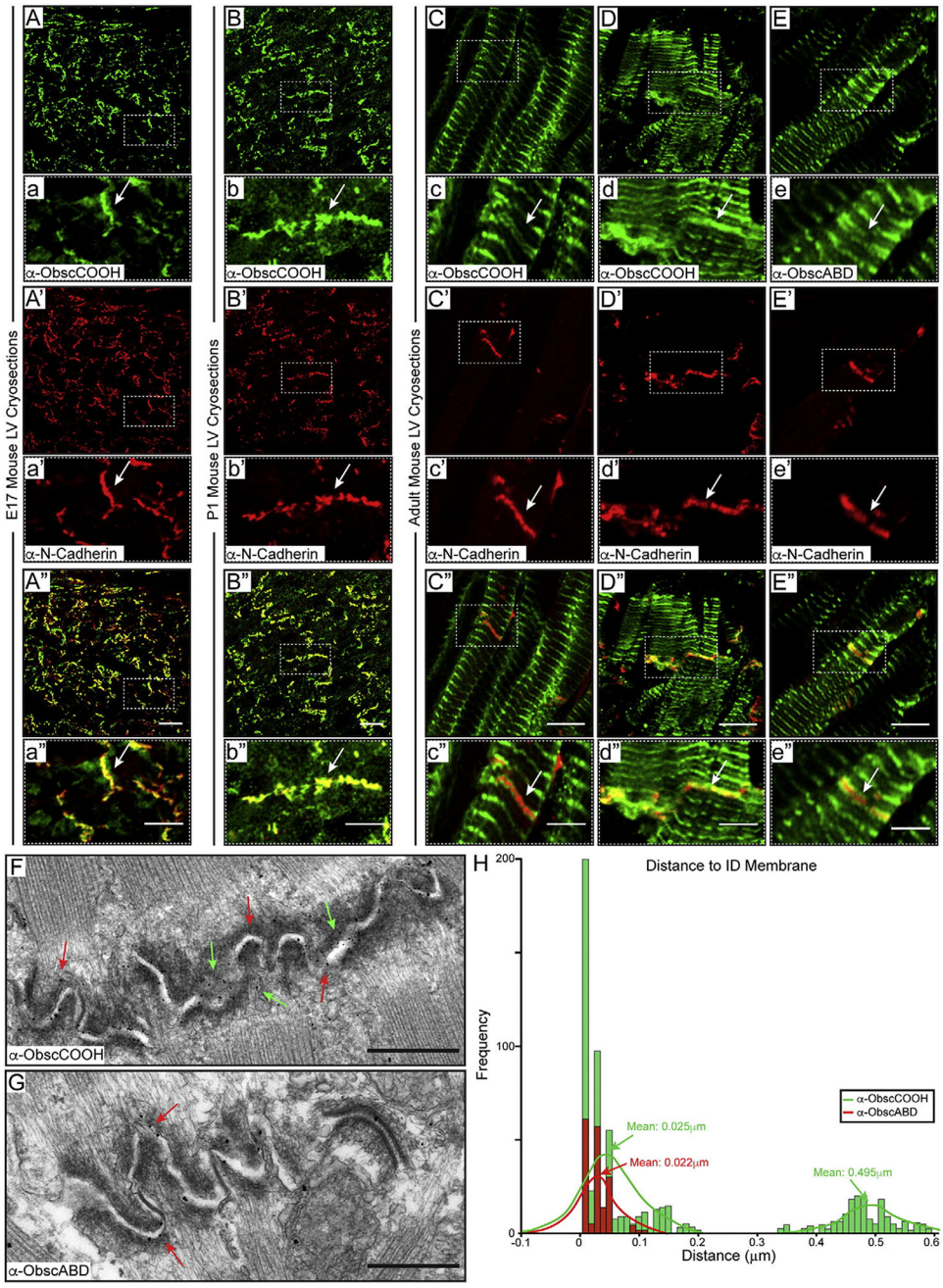

Fig. 2.

Small obscurins −80 and −40 localize to distinct ID subdomains. Cryosections of mouse hearts from embryonic day 17 (A–A″), postnatal day 3 (B–B″), and mature adult myocardium (C–E″) (n = 5 for each group) were sectioned and processed for immunofluorescent staining using α-ObscCOOH (green) and α-N-cadherin (red) antibodies; inset shows zoomed-in images of the boxed areas. Antibodies to the COOH-terminus of obscurins label the ID, coincident with N-cadherin at developmental and mature stages. (C–E″) Notably, we observed two staining patterns for obscurins at the mature ID: i. a broad band (D, arrow) coinciding with the ID membrane where N-cadherin (D′) also resides, and

ii. a doublet flanking the ID membrane (C, arrow) on the edges of N-cadherin staining (D′). Scale bar 20 μm for A″–B″, 10 μm for a″, b″, C″, D″ and E″, and 5 μm for c″, d″ and e″. (F–H) Ultrathin cryo-sections of adult mouse cardiac muscle were labeled with antibodies specific for the COOH-terminus of obscurins, α-obscCOOH (F) and α-obscABD (G). Epitopes recognized by the α-obscCOOH antibody are located in close proximity to the ID membrane at the peaks of the ID folds (red arrows) and within the transition zone between the ID membrane and neighboring sarcomeres (yellow arrows). The α-obscABD antibody, however, only labels close to the ID membrane at the peaks of the ID folds (red arrows). Scale bar 500 nm. (H) The distance of each gold particle from the center of the ID membrane was measured. Measurements are represented as a histogram illustrating the bimodal and single Gaussian distributions of measurements for the α-obscCOOH and α-obscABD antibodies, respectively. The measurements for the α-obscCOOH antibody yielded populations with ~0.5 μm and ~0.02 μm mean distances from the ID membrane, whereas the measurements for the α-obscABD antibody yielded a single population with ~0.02 μm mean distance from the ID membrane (N= 2 hearts and n= 120 IDs per antibody).

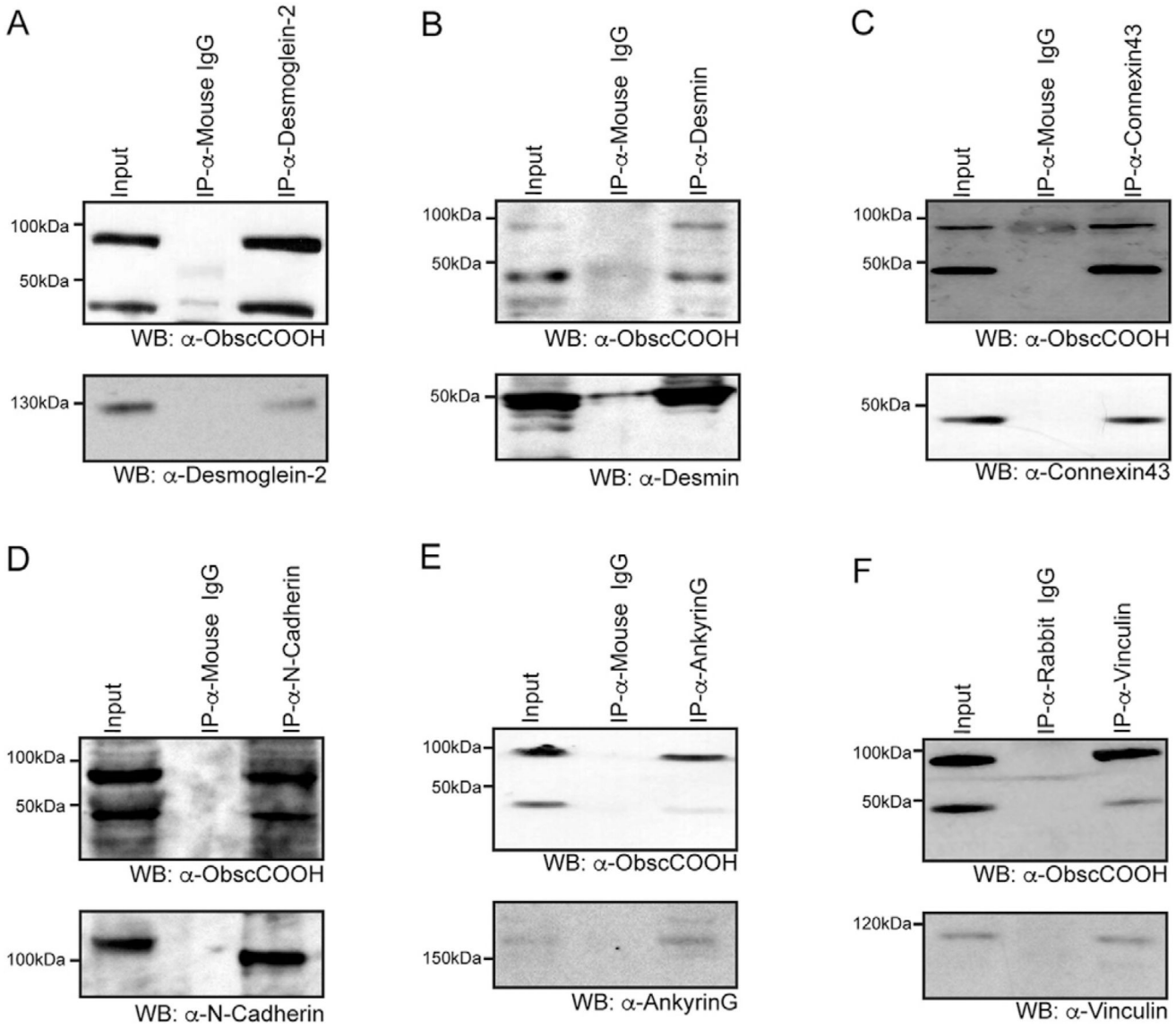

Fig. 3.

Obsc-40 and obsc-80 are in a complex with other ID proteins. Immunoprecipitates using adult mouse lysates and antibodies to desmoglein-2 (A), desmin (B), connexin43 (C), N-cadherin (D), ankyrinG (E), and vinculin (F) indicated that both obsc-80 and obsc-40 exist in complexes with those proteins. Representative blots from 3 independent experiments are shown.

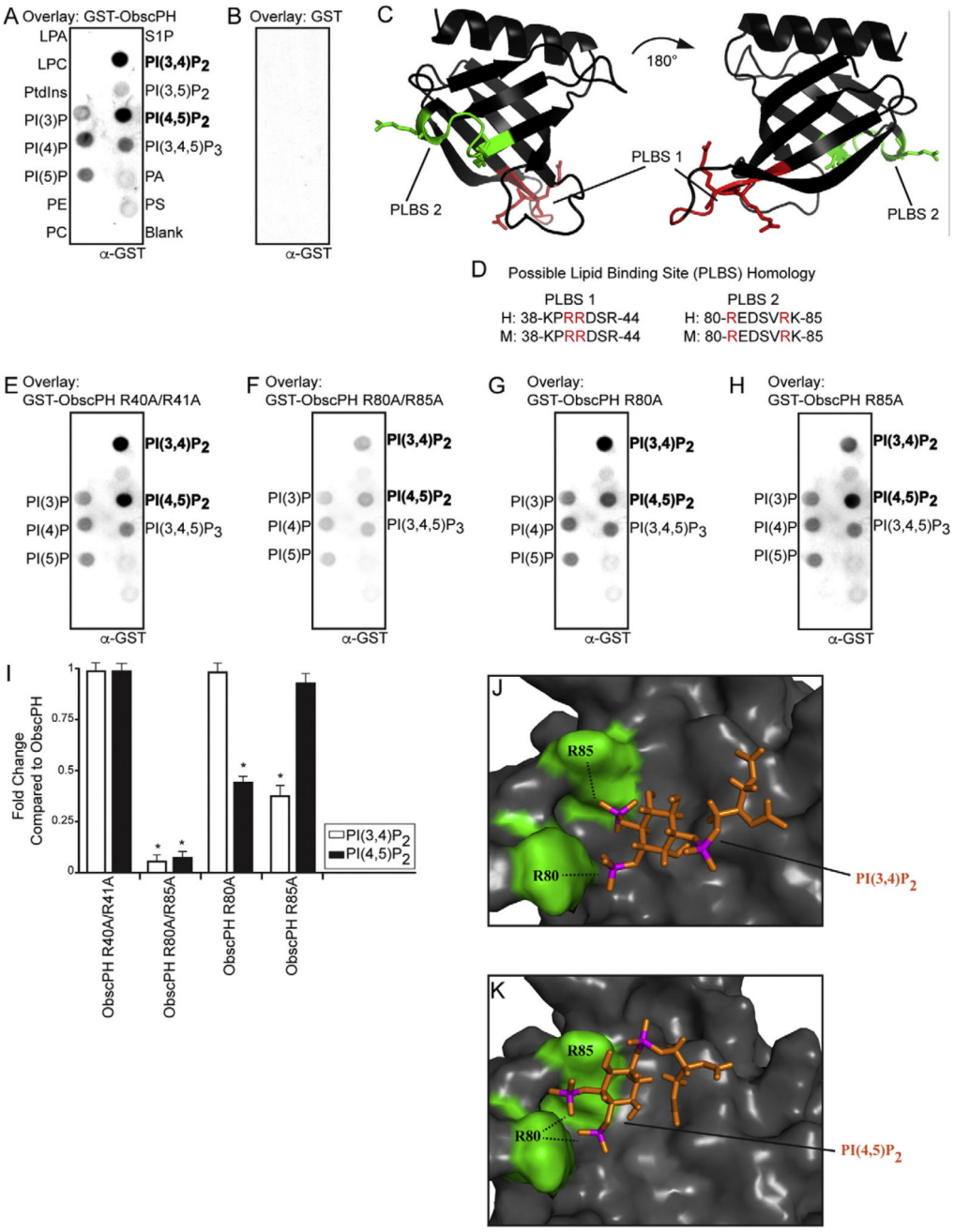

Fig. 4.

The obscurin PH-domain interacts with select PIP2s via residues R80 and R85. Lipid dot-blots using recombinant GST-ObscPH (A) and GST-protein (B) as control indicated that the PH-domain of obscurins interacts directly and strongly with $PI(3,4)P_2$ and $PI(4,5)P_2$ and weakly with $PI(3,4,5)P_3$, PI(3)P, PI(4)P, and PI(5)P. (C–D) Molecular modeling predicted two Possible Lipid Binding Sites (PLBS) on the surface of the obscurin PH-domain, PLBS 1 and PLBS 2. (E–F) Concurrent mutation of residues R40 and R41 within PLBS 1 to alanine (A) failed to alter the lipid binding capacity of the obscurin PH-domain. However, simultaneous mutation of R80 and R85 within PLBS 2 to alanine nearly eliminated binding

to $PI(3,4)P_2$ and $PI(4,5)P_2$. (G–H) Single mutations of R80 or R85 to alanine within PLBS 2 resulted in loss of binding to PI(4,5) and PI(3,4), respectively. (I) The fold-change of the binding capacity of mutant R40A/R41A or R80A/R85A obscurin PH-domain relative to wild-type protein was calculated from 5 independent experiments. Student's *t*-test was performed to determine significance, $p < 0.05$ compared to wild-type control. (J–K) Dynamic molecular modeling was used to observe PLBS 2 with bound $PI(3,4)P_2$ or $PI(4,5)P_2$; dotted lines indicate electrostatic interactions.

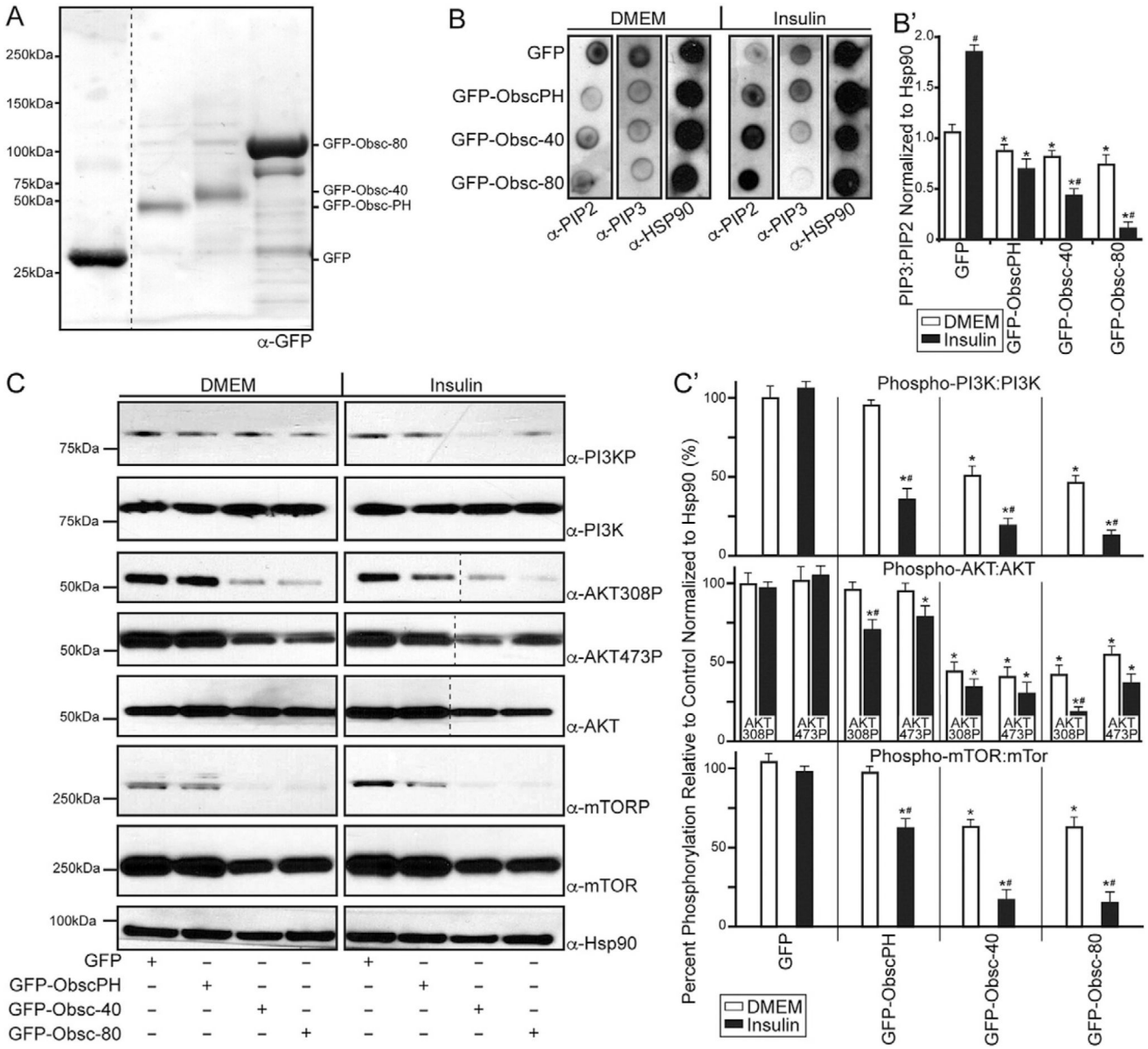

Fig. 5.

Overexpression of obsc-40, obsc-80, and obscurin PH-domain in cardiac cells leads to accumulation of PIP2s, and negatively regulates the PI3K/AKT/mTOR pathway. Obscurin GFP-PH-domain, GFP-obsc-40, GFP-obsc-80, and GFP-protein alone were transiently expressed in H9C2 cardiac-derived cells. (A) Protein lysates prepared from each cell transfection condition were probed with an α-GFP antibody, and showed sufficient overexpression of the indicated transgenes. Following insulin or DMSO vehicle treatment, lysates were prepared and either spotted on a membrane and probed with antibodies to PIP2, PIP3, and HSP90 (loading control) (B) or processed for immunoblotting with the indicated antibodies (C); Hsp90 served as loading control. Overexpression of the obscurin PH-domain, obsc-40, obsc-80, but not GFP alone, resulted in a significant increase in the amounts of PIP2s compared to PIP3 (B′), and a marked decrease in the phosphorylation levels of major

components of the PI3K cascade (C′). The relative expression levels of the indicated proteins were calculated from 5 independent experiments. Two-way ANOVA was performed to determine significance, $p < 0.05$; *significant compared to GFP control transfected myocytes, #significant compared to DMEM corresponding controls. Dashed lines denote discontinuity in the data due to the different order that the samples were loaded in the gel and presented herein.

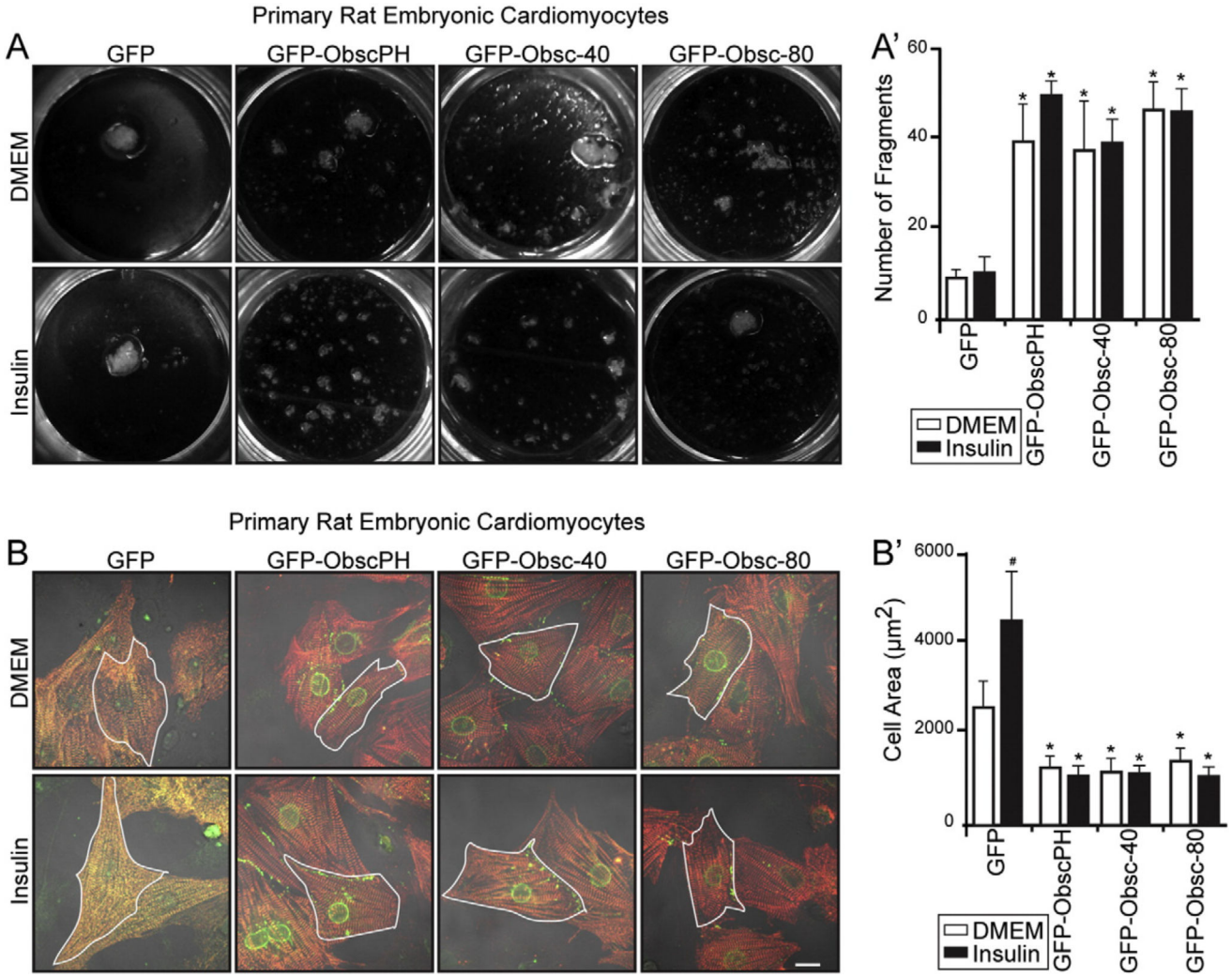

Fig. 6.

Overexpression of obsc-40, obsc-80, and obscurin PH-domain in cardiac cells results in reduced cell adhesion and size. (A–A′) Confluent monolayers of primary RNCM after transient transfection with obscurin GFP-PH-domain, GFP-obsc-40, GFP-obsc-80, or GFP-protein were treated with vehicle DMSO or insulin, and subjected to a dispase mechanical dissociation assay. (A) Representative images of RNCM following dispase mechanical dissociation assay. (A′) Ectopic expression of obscurin PH-domain, obsc-40 and obsc-80 resulted in significantly increased fragmentation compared to control GFP-protein in both DMSO treated and insulin-stimulated cells. Each assay was done in triplicate, 5 independent times, and two-way ANOVA was used to determine significance, $p < 0.05$. (B) Representative overlay images of transmitted light and GFP-fluorescent transfected primary RNCM stained for α-actinin (red) overexpressing control GFP-protein, obscurin PH-domain, obsc-40, or obsc-80 subjected to DMSO vehicle or insulin stimulation (n= 5 independent repeats with 25 cells analyzed for each condition for each repeat). Cellular outline (marked in white) was used to measure cellular area. Scale bar 20 μm. (B′) Quantification of the cellular area indicated that overexpression of the obscurin PH-domain, obsc-40 or obsc-80, but not GFP-alone, led to significant decrease in cell size. Two-way

ANOVA was performed to determine significance, $p < 0.05$, using measurements from five independent experiments; * indicates significance compared to GFP control transfected myocytes, # indicates significant compared to DMEM corresponding controls.

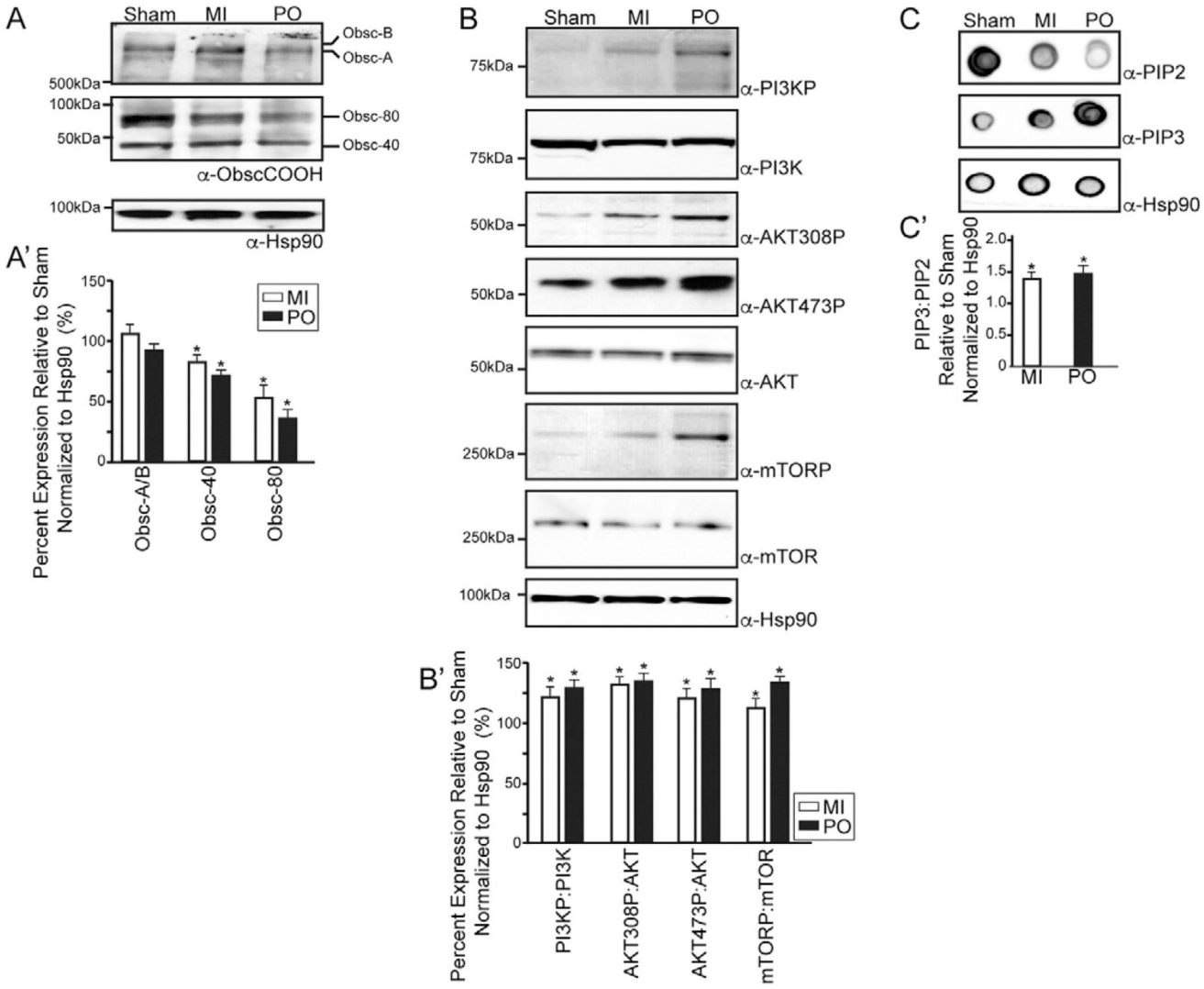

Fig. 7.

Acute and chronic stress heart models exhibit decreased levels of obscurins and increased levels of active PI3k/AKT/mTOR. (A–A′) Lysates of adult mouse hearts subjected to MI, PO, or sham surgery (n = 5 per group) were analyzed via immunoblotting using antibodies to the COOH-terminus of obscurins. (A′) Quantitation of giant and small obscurins' relative expression in MI and PO cardiac models relative to sham controls demonstrated that the levels of obsc-80 and obsc-40, but not giant obsc-A and obsc-B, are significantly reduced in both stress models. (B–B′) The phosphorylation but not total levels of key members of the PI3K/AKT/mTOR cascade were significantly increased in MI and PO hearts compared to sham controls. (C–C′) A significant shift in the ratio of endogenous PIP2:PIP3 toward PIP3 was observed in MI- and PO-stressed hearts compared to controls. The relative expression levels of the indicated proteins were calculated from 5 independent experiments. One-way ANOVA was performed to determine significance, $p < 0.05$. HSP90 was used as loading and normalization control following stripping of the corresponding blot.

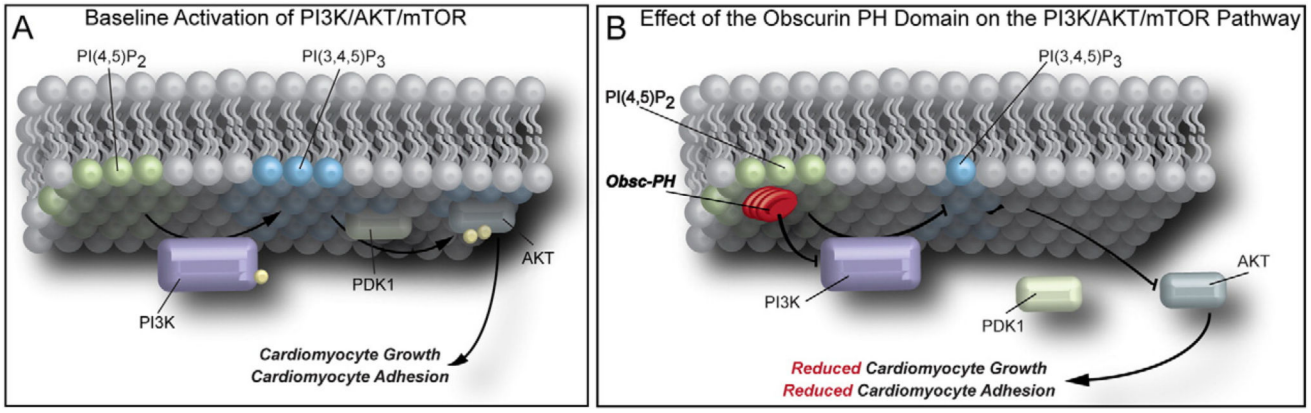

Fig. 8.

Model of the obscurin PH-domain contributing to the regulation of the PI3K/AKT/mTOR pathway. (A) Baseline activation of the PI3K/AKT/mTOR pathway ensures a balanced level of endogenous PIP2s and PIP3s at the membrane. Once activated, phosphorylated PI3K (phosphorylation shown by a yellow sphere) converts PIP2 to PIP3 via the addition of a phosphate group. PIP3s then recruit PDK1 and AKT to the membrane where PDK1 phosphorylates and activates AKT. Activated AKT has a multitude of downstream targets, including mTOR that is a major regulator of cell growth and adhesion. (B) The obscurin-PH domain fine tunes this pathway by acting as a “sink” of PIP2s, limiting their availability for PI3K-mediated phosphorylation, and thus precluding the aberrant activation of the PI3K/AKT/mTOR pathway, which in turn results in regulated cell size and adhesion.